Available online at www.sciencedirect.com
ScienceDirect
Journal of Solid State Chemistry 181 (2008) 325–333
JOURNAL OF SOLID STATE CHEMISTRY
www.elsevier.com/locate/jssc

The influence of phase and morphology of molybdenum nitrides on ammonia synthesis activity and reduction characteristics

D. Mckay[a], J.S.J. Hargreaves[a,*], J.L. Rico[b], J.L. Rivera[b], X.-L. Sun[a,c]

[a]*WestCHEM, Department of Chemistry, Joseph Black Building, University of Glasgow, Glasgow G12 8QQ, UK*
[b]*Laboratorio de Catalisis, Facultad de Ingenieria Quimica, UMSNH, Edificio E, C.U., Morelia Mich., Mexico*
[c]*Department of Chemical Engineering, Shanghai Institute of Technology, 120 Cao Bao Road, Shanghai 200235, PR China*

Received 21 August 2007; received in revised form 15 October 2007; accepted 1 December 2007
Available online 8 December 2007

Abstract

The reactivities of a series of ternary and binary molybdenum nitrides have been compared. Data have been obtained for the catalytic synthesis of ammonia at 400 °C and ambient pressure using a 3:1 H_2:N_2 mixture. Amongst the ternary nitrides, the mass normalised activity is in the order $Co_3Mo_3N > Fe_3Mo_3N \gg Ni_2Mo_3N$. For the binary molybdenum nitrides, the ammonia synthesis activity is significantly lower than that of Co_3Mo_3N and Fe_3Mo_3N and varies in the order γ-$Mo_2N \sim \beta$-$Mo_2N_{0.78} \gg \delta$-MoN. Nanorod forms of β-$Mo_2N_{0.78}$ and γ-Mo_2N exhibit generally similar activities to conventional polycrystalline samples, demonstrating that the influence of catalyst morphology is limited for these two materials. In order to characterise the reactivity of the lattice nitrogen species of the nitrides, temperature programmed reactions with a 3:1 H_2:Ar mixture at temperatures up to 700 °C have been performed. For all materials studied, the predominant form of nitrogen lost was N_2, with smaller amounts of NH_3 being formed. Post-reaction powder diffraction analyses demonstrated lattice shifts in the case of Co_3Mo_3N and Ni_2Mo_3N upon temperature programmed reaction with H_2/Ar. Incomplete decomposition yielding mixtures of Mo metal and the original phase were observed for Fe_3Mo_3N and γ-Mo_2N, whilst β-$Mo_2N_{0.78}$ transforms completely to Mo metal and δ-MoN is converted to γ-Mo_2N.
© 2007 Elsevier Inc. All rights reserved.

Keywords: Molybdenum nitride; Ammonia; Reduction; Structure sensitivity

1. Introduction

Metal nitrides continue to attract interest in terms of their mechanical, optical, magnetic and catalytic properties [1–4]. In the latter case, there has been a resurgent interest since Volpe and Boudart [5] demonstrated that high surface area materials were accessible via ammonolysis of oxide precursors using low-temperature ramp rates and high ammonia space velocities. These parameters are believed to be crucial to the attainment of high surface areas via the minimisation of the partial pressure of water generated during the synthesis. Water is believed to reduce surface area via the effects of hydrothermal sintering. Wise and Markel [6] subsequently showed that, in the case of γ-Mo_2N, N_2/H_2 mixtures could also be successfully employed instead of NH_3 for the synthesis of high surface area materials, again providing very high space velocities and low ramp rates were employed. Indeed, they even argued that N_2/H_2 mixtures were preferable to NH_3 in large-scale synthesis due to the difficulties associated with heat transfer in the endothermic process associated with NH_3.

In terms of the catalytic interest centring on nitrides and oxynitrides, most attention has centred around two main general areas. A number of studies have investigated the application of interstitial nitrides including γ-Mo_2N and Co_3Mo_3N in reactions which are typical of metals, such as those involving hydrogen transfer. In many cases, the use of nitrides in this context has its origins in the perceived similarity of the electronic structures of Mo_2N and precious metals (e.g. [7]). A second general area that has attracted attention is the application of oxynitrides as base catalysts. Oxynitrides are of interest in this area because of

*Corresponding author. Fax: +44 141 330 4888.
E-mail address: justinh@chem.gla.ac.uk (J.S.J. Hargreaves).

0022-4596/$ - see front matter © 2007 Elsevier Inc. All rights reserved.
doi:10.1016/j.jssc.2007.12.001

the ability to control the levels of nitrogen doped into the system, and hence their basicity. Amongst systems in this category having been studied to date are AlVON [8], ZrPON [9] and even nitrogen-containing microporous structures such as aluminophosphates [10] and ZSM-5 [11]. It has generally been argued that the latter classes of material are of great potential in the development of shape-selective microporous base catalysts. The incorporation of low levels of nitrogen within a wide range of oxide hosts is also currently receiving attention in terms of the development of visible light active photocatalysts (e.g. [12]). Our interest in the catalytic chemistry of nitrides and oxynitrides has a different origin from those described above. We are pursuing the possible analogy with the well-established Mars–van Krevelen oxidation mechanism operative in many oxidation reactions catalysed by oxides. In this mechanism, a substrate is directly oxidised by the lattice oxygen of the oxide catalyst, generating transient vacancies which are then replenished by a gas-phase oxygen source. The lattice oxygen of the oxide is therefore reactive and the reaction can also be observed even in the case of non-reducible oxides such as MgO [13], where we have shown isotopic oxygen exchange pathways to be strongly dependent upon the preparation route. In terms of process considerations, the occurrence of this mechanism allows the separation between substrate oxidation and catalyst re-oxidation, which can be beneficial in circumstances where there is the possibility of sequential gas-phase over-oxidation of a desired product [14]. Analogous to oxidation, Mars–van Krevelen-type processes are also observed in the case of sulfur transfer in sulfide catalysts [15] and even for carbide catalysts. In the latter case, Green and co-workers [16] have demonstrated direct lattice carbon transfer to the carbon monoxide produced in the partial oxidation of methane catalysed by molybdenum carbide. The potential occurrence of such pathways occurring within metal nitride catalysts seems to have been largely ignored, despite early reports including those centring upon the uranium nitride catalysed ammonia synthesis in which the importance of interstitial nitrogen was described [17,18]. Very recently, in a TAP reactor-based study, Olea et al. [19] have demonstrated the transfer of lattice nitrogen to the product in the VAlON catalysed direct ammoxidation of propane. Furthermore, based upon the dramatic onset of ammonia decomposition activity of zirconium oxynitride associated with the β'- to β''-phase change, Soerijanto et al. [20] have proposed a mechanism in which part of the product nitrogen originates from the lattice in a catalytic cycle wherein it is subsequently replenished from gas-phase ammonia. In our own work in this area, we have sought to develop a detailed understanding of the reactivity of lattice nitrogen via the comparison of ammonia synthesis rates with N_2/H_2 mixtures and Ar/H_2 mixtures as a function of temperature over a series of interstitial nitrides, with the possibility of re-nitridation in a separate step. The separation of nitridation and de-nitridation steps may have potential merit in the development of novel nitrogen transfer pathways in which NH_3 is used as a nitrogen containing reagent where H_2 loss is thermodynamically limiting. As part of our investigation, we have recently reported on the reaction of Co_3Mo_3N with H_2, where it may be possible to cycle via a Co_6Mo_6N-like phase [21]. Here, we extend that previous investigation to various molybdenum nitride phases and morphologies and Fe_3Mo_3N and Ni_2Mo_3N. Rather than the development of detailed mechanistic understanding for ammonia synthesis, the primary objective of the present study is to determine the influence of structure (i.e. phase and morphology) upon the ammonia synthesis activity and reduction behaviour of materials.

2. Experimental

2.1. Materials preparation

γ-Mo_2N was prepared by ammonolysis of an MoO_3 (Sigma Aldrich, 99.5%) precursor. For nitriding, approximately 1 g of material was held in a vertical quartz reactor into which a $94\,ml\,min^{-1}$ NH_3 (BOC, 99.98%) was introduced. The furnace was programmed to heat the material in three stages. The temperature was increased from ambient to 357 °C at a rate of $5.6\,°C\,min^{-1}$ and then to 447 °C at $0.5\,°C\,min^{-1}$, then to 785 °C at $2.1\,°C\,min^{-1}$ and the furnace was held at this temperature for 5 h. The nitrided material was cooled in flowing ammonia to ambient temperature and upon reaching this temperature, nitrogen was flushed through the system at $100\,ml\,min^{-1}$ to purge the reactor. Then, to prevent bulk oxidation on exposure of the material to air, the material was passivated overnight using a mixture containing $<0.1\%$ O_2.

β-$Mo_2N_{0.78}$ was prepared *in situ* in the fixed bed microreactor used for the activity evaluations. In this procedure, 0.4 g of MoO_3 (Sigma Aldrich, 99.5%) was charged to the reactor and treated with $60\,ml\,min^{-1}$ of a 3:1 H_2:N_2 (BOC, H_2 99.998%, N_2 99.995%) mixture at 700 °C for 2 h. The stoichiometry used for this material has not been determined by us, but is one of a number reported in the literature.

δ-MoN was prepared according to a procedure based upon that detailed by Marchand et al. [22]. In this method 1 g of MoS_2 (Sigma Aldrich, 99%) was loaded into the quartz reactor, the flow of NH_3 was introduced to the reactor at a rate of $94\,ml\,min^{-1}$. The temperature was raised to 785 °C at a heating rate of $15\,°C\,min^{-1}$ and held at this temperature for 60 h to form δ-MoN. The material was then cooled to ambient temperature in flowing ammonia, flushed with nitrogen, and discharged from the reactor.

Nanorod forms of γ-Mo_2N and β-$Mo_2N_{0.78}$ were prepared by procedures identical to those described above, except for the precursor which was MoO_3 with a nanorod morphology. The preparation and characteristics of this form of MoO_3 have been described elsewhere [23].

Co_3Mo_3N was prepared by nitriding a cobalt molybdate hydrate ($CoMoO_4 \cdot nH_2O$) precursor, which was prepared

by adding aqueous solutions of $Co(NO)_3 \cdot 6H_2O$ (Sigma Aldrich, 98 + %) to $(NH_4)_6Mo_7O_{24} \cdot 4H_2O$ (Alfa Aeser, JM 81–83% as MoO_3) and heating the mixed solution to approximately 80 °C. A purple precipitate was obtained after vacuum filtration and the precipitate was washed twice with distilled water and once with ethanol and then dried overnight at 150 °C. The powder was calcined at 500 °C and then nitrided using the procedure detailed above for γ-Mo_2N.

Fe_3Mo_3N and Ni_2Mo_3N were prepared by nitriding the transition metal molybdates, $FeMoO_4$, $NiMoO_4$ according to the procedure carried out by Bem et al. [24]. The transition metal molybdates were prepared by dropwise addition of 400 ml (0.25 M) of an aqueous solution of metal nitrate, $Fe(NO_3)_3 \cdot 9H_2O$ (>98%, Sigma-Aldrich) or $Ni(NO_3)_2 \cdot 6H_2O$ (Sigma-Aldrich), to a 150 ml solution of $Na_2MoO_4 \cdot (H_2O)_2$. A brown (M = Fe) or green (M = Ni) precipitate was obtained after vacuum filtration and the precipitate was washed twice with distilled water and once with ethanol and dried overnight at 150 °C. The powder ($FeMoO_4$/$NiMoO_4$) was then calcined at 700 °C for 6 h under a flow of nitrogen gas (5 ml min^{-1}). The transition metal molybdates were then nitrided according to the general procedure previously described for γ-Mo_2N.

2.2. Activity testing

Reaction studies were performed using 0.4 g of material placed in a silica reactor tube and held centrally between two silica wool plugs within the heated zone of a furnace. All materials were pre-treated at 700 °C with 60 ml min^{-1} of 3:1 H_2:N_2 (BOC, H_2 99.998%, N_2 99.995%) for 2 h. Ammonia synthesis experiments were performed at 400 °C using this gas mixture, following cooling under the reactant gas mixture. The vent gas from the reactor was flowed through 200 ml of a 0.00108 M sulfuric acid solution and the rate of ammonia formation was calculated by determining the rate of change of conductivity with respect to time. H_2/Ar reactions were performed in a similar manner to those for ammonia synthesis, but using a 3:1 H_2:Ar mixture (BOC, H_2 99.998%, Ar min 99.99%) following the 700 °C pre-treatment and subsequent cooling to 400 °C under H_2/N_2.

2.3. Characterisation

Scanning electron microscopy was performed on Philips XLSEM and FEI Quanta 200F Environmental instruments operating at 20 kV.

Powder diffraction analyses were performed using a Siemens D5000 instrument operating with a Cu$K\alpha$ X-ray tube. A 2θ range between 5° and 85° was scanned using a counting rate of 1 s per step with a step size of 0.02°. Samples were prepared by compaction into a Si sample holder.

CHN analysis was performed using an Exeter Analytical CE-440 elemental analyser.

BET surface areas were determined from nitrogen physisorption isotherms measured at liquid nitrogen temperature using a Micromeritics Gemini instrument.

3. Results and discussion

The steady-state rates of ammonia synthesis with a 3:1 H_2:N_2 mixture at ambient pressure and 400 °C for the various nitrides investigated are reported in Table 1. A typical conductivity–time plot from which the rate data are derived is shown in Fig. 1. Figs. 2 and 3 present the post-reaction powder X-ray diffraction samples of the samples tested and confirm the phase assignments made. Generally, except for δ-MoN and Fe_3Mo_3N where a minority γ-Mo_2N phase is formed and Ni_2Mo_3N which contains a minority Ni phase, materials are found to be single phases. For all the data reported in the table, the production of ammonia is far from that expected on the basis of thermodynamic equilibrium. In accordance with previous literature [25–30], Co_3Mo_3N is found to exhibit the highest rate, being greater than that of all the molybdenum nitrides as well as the Fe_3Mo_3N and Ni_2Mo_3N ternary nitrides. Within the literature the activity of Co_3Mo_3N, which can be further enhanced by Cs^+ doping, has been argued to

Table 1
Ammonia synthesis rates of the various nitride catalysts at 400 °C and ambient pressure using a 3:1 N_2:H_2 reaction mixture

Catalyst	NH_3 synthesis rate (μmol h^{-1} g^{-1})
Co_3Mo_3N	167
Fe_3Mo_3N	95
Ni_2Mo_3N	29
γ-Mo_2N	34
β-$Mo_2N_{0.78}$	35
δ-MoN	4
γ-Mo_2N (nanorods)	30
β-$Mo_2N_{0.78}$ (nanorods)	41

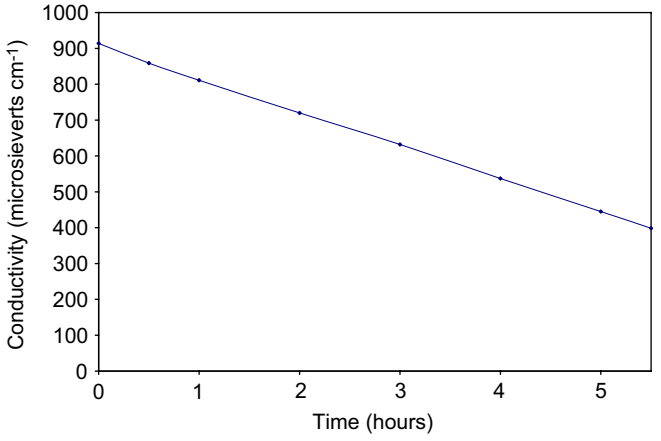

Fig. 1. The change of conductivity as a function of time for the ammonia synthesis reaction over Co_3Mo_3N at 400 °C and ambient pressure using a 3:1 H_2:N_2 mixture.

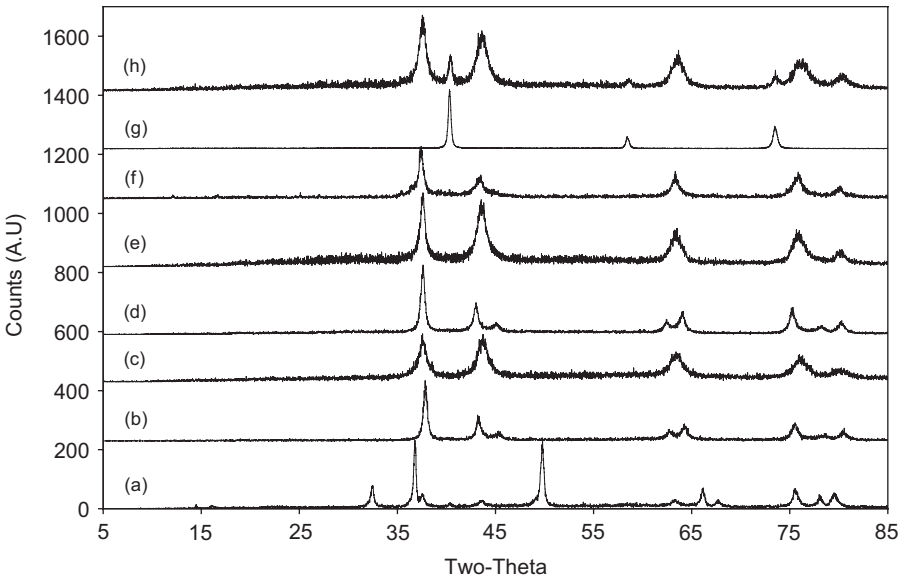

Fig. 2. Powder X-ray diffraction patterns of the binary molybdenum nitrides: (a) δ-MoN, (b) β-$Mo_2N_{0.78}$, (c) γ-Mo_2N, (d) β-$Mo_2N_{0.78}$ nanorods, (e) γ-Mo_2N nanorods, (f) δ-MoN following temperature-programmed reaction with Ar/H_2 up to 700 °C, showing its transformation into γ-Mo_2N, (g) β-$Mo_2N_{0.78}$ following temperature programmed reaction with Ar/H_2 up to 700 °C following showing its transformation into Mo metal and (h) γ-Mo_2N following temperature-programmed reaction with Ar/H_2 up to 700 °C showing its partial conversion into Mo metal.

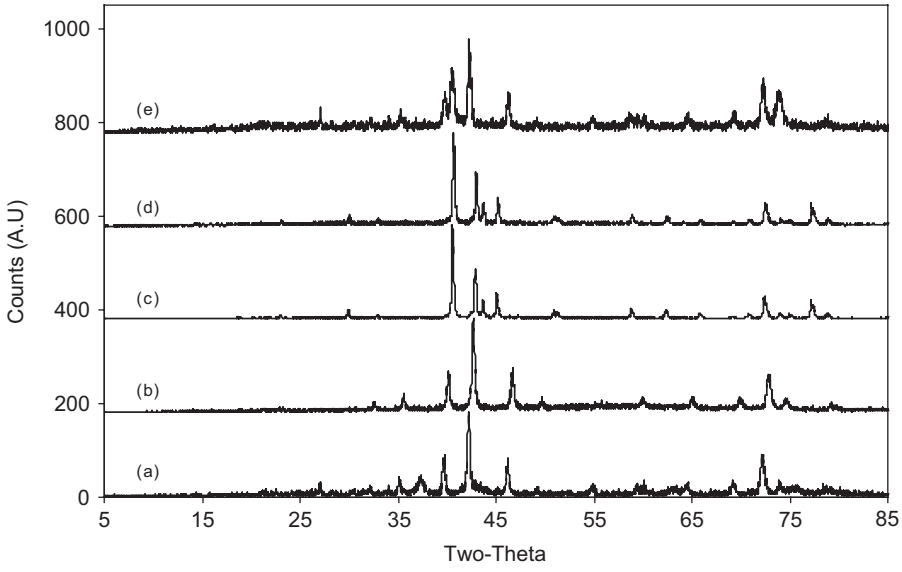

Fig. 3. Powder X-ray diffraction patterns of the ternary molybdenum nitrides: (a) Fe_3Mo_3N, (b) Co_3Mo_3N, (c) Ni_2Mo_3N, (d) Ni_2Mo_3N following temperature-programmed reaction with Ar/H_2 up to 700 °C, where the general form of the pattern is retained but there are small shifts in the positions of the reflections to higher angle, and (e) Fe_3Mo_3N following temperature-programmed reaction with Ar/H_2 up to 700 °C which partially decomposes to yield Mo metal, with the remaining Fe_3Mo_3N phase showing no shift in the position of its reflections.

arise as a consequence of a synergistic combination of Co and Mo components generating optimum nitrogen-binding strength, with the role of the nitrogen within the structure being the stabilisation of the active (111) lattice plane [31]. On this basis, in which Fe_3Mo_3N and Ni_2Mo_3N would be expected therefore to have non-optimal binding strengths (with iron being stronger than cobalt, and nickel weaker than cobalt [31,32]) it may be possible to rationalise their lower activity.

Despite their relatively low activity, it is interesting to make comparisons between the various binary nitride polymorphs. To our knowledge, although molybdenum nitride is a relatively active ammonia synthesis catalyst, such comparisons have not been widely made. In general, most studies of the catalytic properties of molybdenum nitrides have centred upon the γ-Mo_2N phase, which is the most commonly synthesised. It is worth noting that Kojima and Aika [33] have reported the activity of a

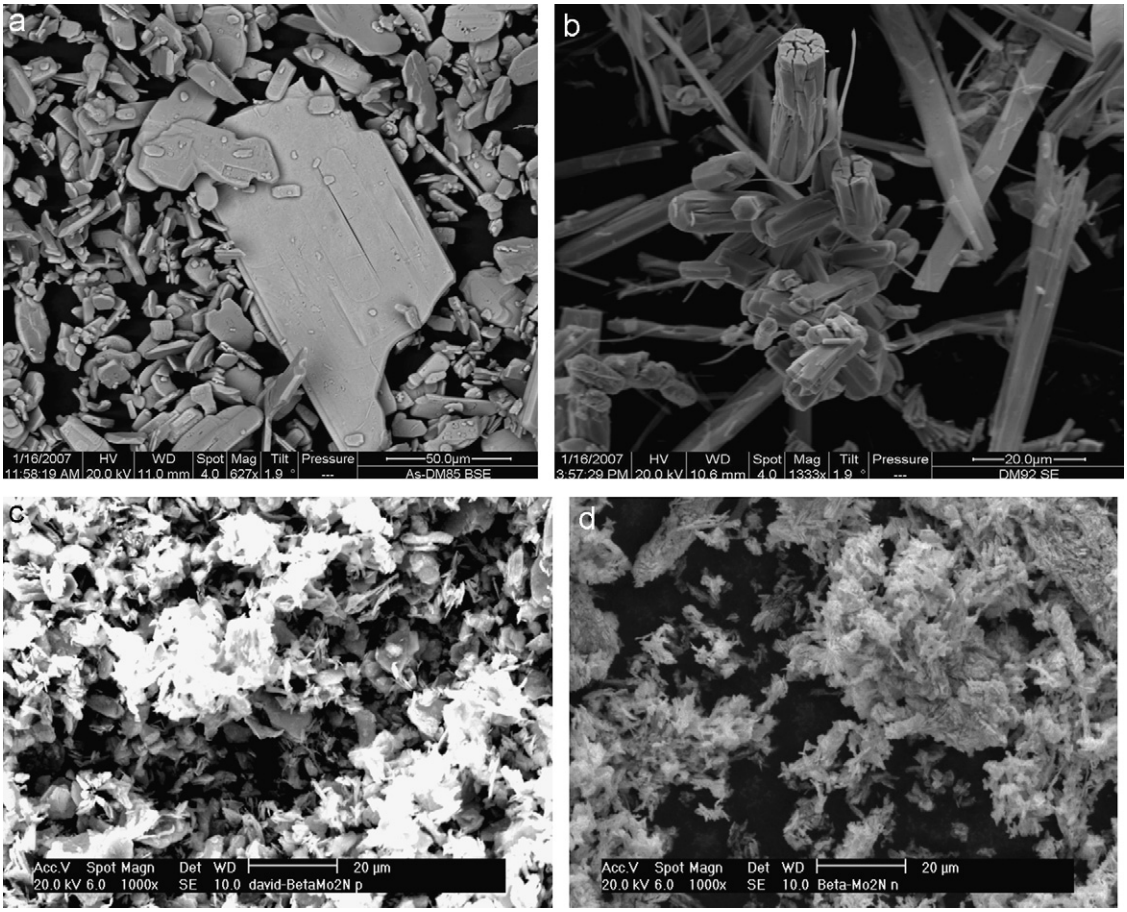

Fig. 4. SEM micrographs of (a) γ-Mo_2N prepared from MoO_3 powder; (b) γ-Mo_2N nanorods; (c) β-$Mo_2N_{0.78}$ prepared from MoO_3 powder; and (d) β-$Mo_2N_{0.78}$ prepared from MoO_3 nanorods.

γ-Mo_2N ammonia synthesis catalyst to be 48 $\mu mol\,h^{-1}\,g^{-1}$ under conditions comparable to ours. On inspection of the table, whilst it is apparent that all these catalysts have low activity in relation to Co_3Mo_3N, there are pronounced differences between them. The mass normalised activity of β-$Mo_2N_{0.78}$ is found to be similar to that for γ-Mo_2N, which, in turn, is significantly greater than that for δ-MoN. Since the samples are air sensitive, are passivated prior to reaction, and react with air on discharge from the reactor, the pre- and post-reaction BET surface areas measured may not be fully representative of the area exhibited by reacting samples. However, post-reaction analysis indicates the specific area of β-$Mo_2N_{0.78}$ ($9\,m^2\,g^{-1}$) to be about a tenth of that of γ-Mo_2N ($85\,m^2\,g^{-1}$), which indicates that the former material has a much greater surface area normalised activity. Indeed, even on this basis, δ-MoN ($18\,m^2\,g^{-1}$) has by far the lowest activity, although in this material the potential adverse influence of sulfur residues cannot be absolutely excluded. β-$Mo_2N_{0.78}$, γ-Mo_2N and δ-MoN present very different crystal structures. γ-Mo_2N can be viewed of as a face centred cubic arrangement of molybdenum atoms with nitrogen atoms distributed within one-half of the resultant octahedral interstitial sites [34], whereas β-$Mo_2N_{0.78}$ is based on a body centred tetragonal unit cell [1], and δ-MoN possesses the NiAs structure [22]. It is clear that, in addition to their structure, there are pronounced differences in stoichiometry between the various phases. Indeed, one route to β-$Mo_2N_{0.78}$ is via the high-temperature transformation of γ-Mo_2N by loss of N_2 under an inert atmosphere. However, in terms of catalytic activity, the surface structure, which is not probed in powder diffraction, is of prime significance. In this context, it is important to note that Thompson and co-workers [35] have reported the surface structure of passivated γ-Mo_2N, which was argued to be representative of the nitrided surface, to be a body centred phase. On this basis, it is possible that the surface phases do not directly correspond to the bulk ones and, although the bulk structures of the phases are very different, their surface structures may not be.

In their investigation of the activity of γ-Mo_2N catalysts of varying surface area, Volpe and Boudart [36] concluded that there was structure sensitivity, with lower surface area catalysts having higher intrinsic activity. Accordingly, we have sought to examine the influence of morphology on catalytic activity and have prepared "nanorod" forms of γ-Mo_2N and β-$Mo_2N_{0.78}$. Post-reaction powder diffraction patterns of the samples are given in Fig. 2 and confirm the phase assignments made. Representative SEMs of the different catalyst morphologies are shown in Fig. 4. It can

Table 2
Nitrogen content of various nitrides following H_2/N_2 reaction at 400 °C and temperature-programmed reaction with H_2/Ar at 700 °C using the regimes shown in Fig. 5

Sample	Stoichiometric nitrogen content (wt%)	Post-N_2/H_2 400 °C reaction nitrogen (wt%)	Post-Ar/H_2 700 °C reaction nitrogen (wt%)	% of N lost attributed to NH_3
Fe_3Mo_3N	2.98	3.52	1.97	22.03
Ni_2Mo_3N	4.33	2.57	2.33	34.15
γ-Mo_2N	6.80	5.78	2.93	19.94
β-$Mo_2N_{0.78}$	5.39	5.70	0	6.78
δ-MoN	12.74	13.33	5.68	3.16

be seen that γ-Mo_2N prepared from MoO_3 powder exhibits plate-like crystals with a large size distribution. The nanotubular γ-Mo_2N also exhibits a wide distribution of crystallite sizes and aspect ratios, and is pseudomorphic with its precursor [23]. Some degree of crystallite fracturing is also evident. This is consistent with the corresponding powder diffraction pattern in Fig. 2 where the reflection widths indicate that the crystallites are multidomainic since, for example, if the (111) width is assumed solely to arise from Scherrer broadening this would correspond to a diffraction domain size of ca. 140 Å, a value clearly much smaller than the apparent crystallite dimensions evident in Fig. 4(b). However, there is a pronounced reflection width anisotropy (compare the patterns for γ-Mo_2N presented in Figs. 2(c) and (e)), which is indicative of acicular morphology of diffraction domains. The retention of morphology on nitridation of oxides to form γ-Mo_2N is well documented in the literature (e.g. [37]). On inspection of the micrographs of the β-$Mo_2N_{0.78}$ phase, it can be seen that the sample formed from the standard MoO_3 powder precursor also exhibits a plate-like morphology, although in this case the morphology is less well-defined and takes on a rougher appearance. The same general observation is true for the nanorod MoO_3-derived sample, although there are rods present that are less well-defined than for the corresponding γ-Mo_2N sample. Inspection of the powder diffraction patterns of the β-phase samples shows that the reflection widths are generally narrower than for their γ-phase counterparts, which is a result of larger diffraction domains and/or a lower degree of disorder. The preparation of the β-phase has been effected by the *in-situ* treatment of the MoO_3 precursors with the H_2/N_2 reaction mixture using a non-controlled temperature ramp rate. Unlike the ammonolysis procedure adopted for the synthesis of γ-Mo_2N, it is anticipated that transient high partial pressures of water will ensue, possibly resulting in the irregular morphology observed.

Ammonia synthesis rates for the nanorod-derived samples are presented in Table 1. Although the β-phase is more active than its powder-derived counterpart on a mass normalised basis, the difference between the two phases and the different morphologies is relatively small and therefore the influence of structure sensitivity in this context is limited.

In order to assess the reactivity of lattice nitrogen within the nitrides, temperature programmed reaction with Ar/H_2 has been performed, as described elsewhere. In the case of Co_3Mo_3N we observed that ~50% of the nitrogen could be removed in this system by employing the temperature programmed procedures adopted here [21]. Furthermore, in comparative experiments with Ar and Ar/H_2 feeds, hydrogen was shown to be essential for this, despite the fact that the majority of the nitrogen lost from the nitride did not end up in the form of NH_3, presumably as a consequence of the NH_3 dissociation equilibrium at the higher reaction temperatures employed. Accordingly, we have undertaken similar studies with the different binary and ternary phases described in this study. Conductivity data are shown in Fig. 5, whilst post-reaction diffraction patterns are given in Figs. 2 and 3 and CHN analyses in Table 2. Also included in the table are calculated nitrogen contents based upon the stoichiometry of the various materials. It is obvious that there are significant deviations in post 400 °C N_2/H_2 reactions from those expected on the basis of stoichiometry. It is probable that their origin is the presence of sorbed NH_x species in those materials exhibiting greater quantities of nitrogen, such as β-$Mo_2N_{0.78}$, and surface oxidation on subsequent exposure to air for those with lower contents, such as γ-Mo_2N. It is again apparent that, despite the low levels of nitrogen loss as ammonia in the Ar/H_2 reduction sequences, as detailed in Table 2, substantial lattice nitrogen is removed from the structures. The conductivity plots provide information on the temperature dependence of ammonia formation via hydrogenation of the nitride materials. Whilst, as also detailed in Table 2, in all samples the vast majority of nitrogen which is eliminated is not lost in the form of NH_3, the elimination of NH_3 from samples may be an important consideration in terms of one of our main objectives, which is to effect novel catalytic nitrogen transfer reactions via the trapping of intermediate NH_x species by acceptor molecules. For example, it can be seen from the plots that β-$Mo_2N_{0.78}$ slowly eliminates low levels of NH_3 over the entire temperature range investigated, whereas δ-MoN only eliminates NH_3 at temperatures above 400 °C. The diminution of NH_3 loss, sometimes observed with increasing temperature, can be indicative of the depletion of a finite pool of reactive nitrogen species, which are not replenished in the absence of a source of gas-phase nitrogen, or the increasing favourability of ammonia decomposition with temperature.

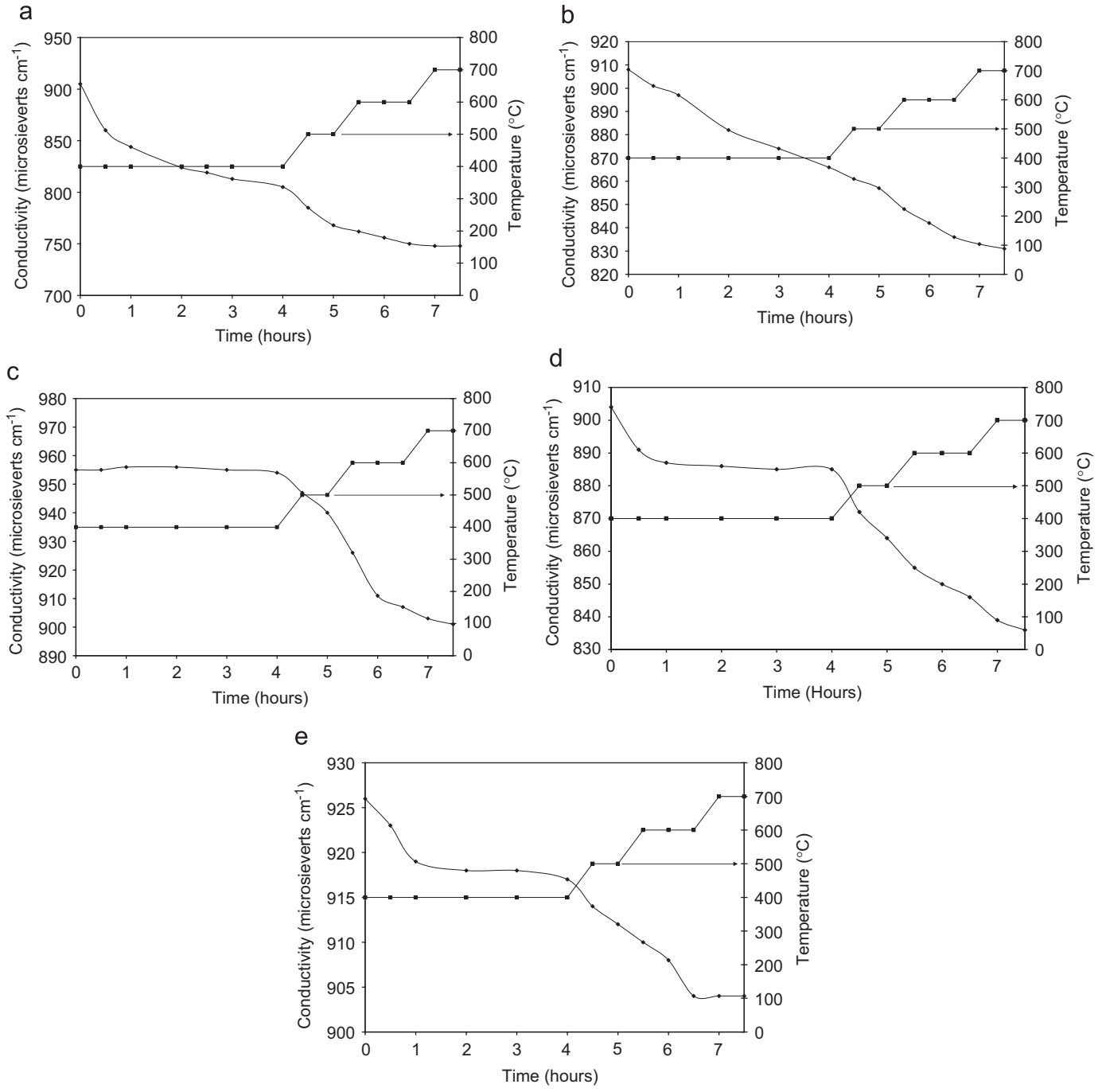

Fig. 5. Conductivity–time plots for temperature-programmed reactions carried out using H_2/Ar: (a) γ-Mo_2N, (b) β-$Mo_2N_{0.78}$, (c) δ-MoN, (d) Fe_3Mo_3N and (e) Ni_2Mo_3N.

The loss of structural nitrogen is also evidenced in the post-Ar/H_2 reaction XRD patterns presented in Figs. 2 and 3. It can be seen that different types of "decomposition" pathway are exhibited. γ-Mo_2N and Fe_3Mo_3N are similar in that the original phase is partly retained, with essentially no change in lattice parameter. However, there are additional reflections in the powder diffraction pattern which become apparent after reaction—in both cases these correspond to the presence of Mo metal and in the latter case this is consistent with the presence of the molybdenum nitride impurity phase. It is interesting to note that we did not evidence the β-phase as an intermediate in the decomposition of γ-Mo_2N (Mo metal possesses a body centred cubic unit cell). This type of behaviour in that part of the sample is totally reduced whereas the remainder apparently has not reduced at all, is intriguing. In all cases, the quantity of hydrogen passed over the nitride samples whilst they are held at 700 °C, the highest temperature employed, is in large excess of that required to totally reduce the samples. Therefore, whilst only a fraction of the

crystallites reduce, it would appear that once reduction is initiated within a crystal it rapidly propagates throughout the crystallite resulting in total elimination of nitrogen from the structure, whilst reduction is not initiated in other crystallites. It is interesting to note that, in the case of γ-Mo_2N, the resultant Mo metal formed has a comparatively narrow reflection width, which may indicate that it is derived from the larger crystals. The behaviour of Ni_2Mo_3N upon nitrogen loss is more similar to, but much less pronounced than, Co_3Mo_3N [21] in that a shift of lattice parameter is observed, indicating the general maintenance of the phase but elimination of structural nitrogen. The shifted Ni_2Mo_3N phase has a lattice parameter of 6.611 Å compared to 6.634 Å reported in the literature for the stoichiometric phase [38], and that for shifted Co_3Mo_3N is 10.879 Å compared to 11.027 Å reported for the stoichiometric phase [39]. δ-MoN, which possesses the NiAs structure type and can therefore be described in terms of hexagonal close packing of Mo atoms, is observed to lose half its structural nitrogen and transform into the face centred cubic-based γ-Mo_2N polymorph.

Currently, the origin of the differences in the types of decomposition pathway, and their determining influences, are not clear. However, the loss of nitrogen, and hence its potential for reaction, is evident. Despite the vast excess of hydrogen in the gas phase, in all cases the predominant form of lost nitrogen is as N_2. This is, we believe, a consequence of the favourable thermodynamics of ammonia decomposition at the higher reaction temperatures employed. The relative proportions of N_2 and NH_3 lost from the materials is a function both of the temperature at which nitrogen is eliminated and also of their catalytic efficacy for ammonia decomposition. In general, within each subset of materials (i.e. binary and ternary), it does seem possible to discern a relationship, possibly fotuitous, between the loss of lattice nitrogen at 400 °C and the NH_3 synthesis activity, which is also measured at 400 °C.

4. Conclusions

In this study, we have made a comparison of various binary and ternary nitrides in terms of their ambient pressure ammonia synthesis activity and their reducibility. Amongst the binary nitrides, it is apparent that the ammonia synthesis activity of the γ- and β-molybdenum nitride phases is comparable on a mass normalised basis with the δ-phase exhibiting a comparatively low activity. Furthermore, when the influence of surface area is taken into account the β-phase is by far the most active. This implies that the lengthy temperature programmed ammonolysis reaction frequently applied to synthesise the γ-phase produces an ammonia synthesis catalyst which, at best, has no advantage to one prepared by direct reaction of the oxide precursor with H_2/N_2. The influence of catalyst morphology on reaction performance has been investigated and has been found to exert little effect. In accordance with previous literature, Co_3Mo_3N has been found to exhibit the highest activity amongst the ternary nitrides investigated. It is significantly more active than all the binary nitrides investigated. The reducibility of the nitrides has also been investigated by temperature programmed reduction with H_2/Ar. Amongst the binary nitrides, β-$Mo_2N_{0.78}$ is observed to be the most easily reduced phase, going completely to the metallic form under conditions which totally transform δ-MoN to the γ-Mo_2N phase and which partially transform the γ-Mo_2N phase to Mo metal. The favourable ammonia synthesis activity is possibly a consequence of the comparative ease of reduction of the β-phase. Amongst the ternary nitrides, Ni_2Mo_3N, which possesses the β-Mn structure, shows the lowest degree of reduction, which may be consistent with its low ammonia synthesis activity, being comparable to those of the γ- and β-phase binary molybdenum nitrides. The lowest activity binary nitride, δ-MoN, does not eliminate NH_3 on Ar/H_2 treatment at 400 °C, the temperature examined for ammonia synthesis.

Acknowledgments

J.S.J.H. and D.M. wish to acknowledge the EPRSC and Crystal Faraday for financial support in the area of nitride catalysis (GR/S87300/01). The kind assistance of Mrs. Kim Wilson in performing CHN analysis is gratefully acknowledged.

References

[1] S.T. Oyama (Ed.), The Chemistry of Transition Metal Carbides and Nitrides, Blackie Academic and Professional, Glasgow, 1996.
[2] D.H. Gregory, J. Chem. Soc. Dalton Trans. 259 (1999).
[3] J.S.J. Hargreaves, D. Mckay, Catalysis Specialist Periodic Report 19, 2006, p. 83.
[4] M. Nagai, Appl. Catal. A: Gen. 322 (2007) 178.
[5] L. Volpe, M. Boudart, J. Solid State Chem. 59 (1985) 332.
[6] R.S. Wise, E.J. Markel, J. Catal. 145 (1994) 335.
[7] S.T. Oyama, G.L. Haller, Catalysis Specialist Periodic Report 5, 1982, p. 333.
[8] H. Wiame, L. Bois, P. L'haridon, Y. Laurent, P. Grange, J. Eur. Ceram. Soc. 17 (1997) 2017.
[9] N. Fripiat, P. Grange, J. Mater. Sci. 34 (1999) 2057.
[10] S. Ernst, M. Hartmann, S. Sauerbeck, T. Bongers, Appl. Catal. A: Gen. 200 (2000) 117.
[11] C. Zhang, Z. Xu, K. Wan, Q. Liu, Appl. Catal. A: Gen. 258 (2004) 55.
[12] R. Asahi, T. Morikawa, T. Ohwaki, K. Aoki, Y. Taga, Science 29 (2001) 269.
[13] A. Burrows, S. Coluccia, J.S.J. Hargreaves, R.W. Joyner, C.J. Kiely, G. Martra, I.M. Mellor, M. Stockenhuber, J. Catal. 234 (2005) 14.
[14] G.E. Keller, M. Bhasin, J. Catal. 73 (1982) 9.
[15] P. Tetenyi, in: J.S.J. Hargreaves, S.D. Jackson, G. Webb (Eds.), Isotopes in Heterogeneous Catalysis, Imperial College Press, London, 2006 (Chapter 4).
[16] T. Xiao, A. Hanif, A.P.E. York, Y. Nishizaka, M.L.H. Green, Phys. Chem. Chem. Phys. 4 (2002) 4549.
[17] N. Segal, F. Sebba, J. Catal. 8 (1967) 105.
[18] N. Segal, F. Sebba, J. Catal. 8 (1967) 113.
[19] M. Olea, M. Florea, I. Sack, R. Prada Silvy, E.M. Gaigneaux, G.B. Marin, P. Grange, J. Catal. 232 (2005) 152.

[20] H. Soerijanto, C. Rodel, U. Wild, M. Lerch, R. Schomacker, R. Schlogl, T. Ressler, J. Catal. 250 (2007) 19.
[21] D. Mckay, D.H. Gregory, J.S.J. Hargreaves, S.M. Hunter, X.-L. Sun, Chem. Commun. 3051 (2007).
[22] R. Marchand, F. Tessier, F.J. Di Salvo, J. Mater. Chem. 9 (1999) 297.
[23] M.A. Albiter, R. Huirache-Acuna, F. Paraguay-Delgado, J.L. Rico, G. Alonso-Nunez, Nanotechnology 17 (2006) 3473.
[24] D.S. Bem, C.P. Gibson, H.-C. Zur Loye, Chem. Mater. 5 (1993) 397.
[25] R. Kojima, K.-I. Aika, Chem. Lett. 514 (2000).
[26] R. Kojima, K.-I. Aika, Appl. Catal. A: Gen. 215 (2001) 149.
[27] R. Kojima, K.-I. Aika, Appl. Catal. A: Gen. 218 (2001) 121.
[28] R. Kojima, K.-I. Aika, Appl. Catal. A: Gen. 219 (2001) 157.
[29] C.J.H. Jacobsen, Chem. Commun. 1057 (2000).
[30] A. Boisen, S. Dahl, C.J.H. Jacobsen, J. Catal. 208 (2002) 180.
[31] C.J.H. Jacobsen, S. Dahl, B.S. Clausen, S. Bahn, A. Logadottir, J.K. Norskov, J. Am. Chem. Soc. 123 (2001) 8405.
[32] A. Ozaki, K. Aika, in: J.R. Anderson, M. Boudart (Eds.), Catalysis Science and Technology, vol. 1, Springer, Berlin, 1981, p. 87 (Chapter 3).
[33] R. Kojima, K.-I. Aika, Appl. Catal. A: Gen. 219 (2001) 141.
[34] C.L. Bull, T. Kawashima, P.F. McMillan, D. Machon, O. Shebanova, D. Dalsenberger, E. Soignard, E. Takayama-Muromachi, L.C. Chapan, J. Solid State Chem. 179 (2006) 1762.
[35] J.G. Choi, J.R. Brenner, C.W. Coiling, B.G. Demczyk, J.L. Dunning, L.T. Thompson, Catal. Today 15 (1992) 201.
[36] L. Volpe, M. Boudart, J. Phys. Chem. 90 (1986) 4874.
[37] C.H. Jaggers, J.N. Michaels, A.M. Stacy, Chem. Mater. 2 (1990) 150.
[38] K.S. Weil, P.N. Kumar, J. Grins, J. Solid State Chem. 146 (1999) 22.
[39] S.K. Jackson, R.C. Layland, H.C. zur Loye, J. Alloys Compd. 291 (1999) 94.